Front. Optoelectron. 2019, 12(3): 249–267
https://doi.org/10.1007/s12200-018-0857-2

REVIEW ARTICLE

# Development of optical-thermal coupled model for phosphor-converted LEDs

**Xinglu QIAN[1], Jun ZOU (✉)[1,2], Mingming SHI[1], Bobo YANG[1], Yang LI[3], Ziming WANG[3], Yiming LIU[3], Zizhuan LIU[1], Fei ZHENG[1]**

1 School of Science, Shanghai Institute of Technology, Shanghai 201418, China
2 Zhejiang Emitting Optoelectronic Technology Co, Ltd., Zhejiang 314100, China
3 School of Material Science and Engineering, Shanghai Institute of Technology, Shanghai 201418, China



**Abstract** In this review, first, we discussed the effect of phosphor features on optical properties by the software simulation in detail. A combination of these parameters: phosphor material, phosphor particle size and particle distribution, phosphor layer concentration, phosphor layer thickness, geometry, and location of the phosphor layer, will result in the final optical performance of the phosphor layer. Secondly, we introduced how to improve light extraction efficiency with various proposed methods. Thirdly, we summarized the thermal models to predict the phosphor temperature and the junction temperature. To stabilize the optical performance of phosphor-converted light emitting diodes (PC-LEDs), much effort has been made to reduce the junction temperature of the LED chips. The phosphor temperature, a critical reliability concern for PC-LEDs, should be attracted academic interest. Finally, we summed up optical-thermal coupled model for phosphors and summarized future optical- thermal issues exploring the light quality for LEDs. We foresee that optical-thermal coupled model for PC-LEDs should be paid more attention in the future.

**Keywords** phosphor-converted light emitting diodes (PC-LEDs), optical-thermal coupled model, software simulation

## 1 Introduction

Since Edison's bulb invented in 1879, lighting engineering has developed rapidly in the past few decades. And improving output power and reducing the size is the tendency with the series evolution of lights [1–5]. On account of the long lifetime, energy savings, environment-friendly characteristics, wide color temperatures, quick startup, light emitting diode (LED) has penetrated into every aspect of daily life, including automobile headlamps, street lamps and general lighting [6–9]. Since LED will benefit society even more widely and deeply in the future, three scientists gained the Nobel Prize in physics in 2014 for inventing efficient blue LEDs based on GaN [10].

There are three methods that are available to realize white LED. The first method is to combine three monochromatic LED showing red, green and blue [11]. However, this method of color mixing brought about low efficiency because of the poor radiant efficiency of green light sources [12,13]. In addition, the different degradation dynamic and temperature management of each light source will result in the color shift during working. Recalibrating mechanism to adapt the color mixing is a way to avoid this problem [14]. But this way makes the system more costly and complex. The second method is the near-ultraviolet (N-UV) LED chips exciting the blue, green, and red phosphor, which changes the wavelength of incident light [15,16]. The third method is using the blue LED to exciting single-phased yellow phosphor or mixed green and red phosphors. This way is practical applications and the major approach in the academic studies [11]. As the third method, the package way for phosphor layer coated on the structure is called phosphor-converted LEDs (PC-LEDs). However, optical energy loss will happen during the process of color conversion, which including light absorption, Stokes shift, and the non-unity quantum efficiency of phosphors particles. The loss of optical energy is converted into heat which can increase the chip junction temperature and the phosphor temperature.

Temperature is the key factor in LEDs system which will influence the lifetime, the luminance output and the

Received July 27, 2018; accepted October 8, 2018

E-mail: zoujun@sit.edu.cn

correlated color temperature (CCT) [17,18]. What's more, more than 60% of the electronic power is generated into heat because of non-radioactive recombination of electron-hole pairs, absorption of back-scattered light and low light extraction [19]. Generally, the heat generated by phosphor compared to the heat generated by chip is quite small. Yan et al. [19] revealed that phosphor temperature is a critical factor affecting the lifetime and the performance of LEDs. Luo et al. [20] claimed that the maximum phosphor temperature can attain 315.9°C, leading to the phosphor quenching even silicone carbonization. To sum up, high phosphor temperature will induce the local stress, material property deterioration. Then it will result in the reduction of the phosphors quantum conversion efficiency and the decrease of luminous efficiency attributed to the thermal quenching effect. Consequently, effects on the photometric electric and thermal performance of the PC-LEDs device need more studies. Thermal model is regarded as an effective tool to predict temperature for PC-LEDs device. Moreover, part of the light is absorbed by the packaging material and converted into heat during the process of optical propagation. Well-designed optical components and optical interface structure also play an important role in reducing the light absorption in the packaging material loss.

Recently, numerous studies have been reported on the optical design for reducing the light absorption, refraction, scattering, and reflection. Similarly, researchers all over the world have conducted plenty of research on the thermal model. Also, there are several outstanding reviews on the LEDs phosphors development. However, the development of optical-thermal coupled model for PC-LEDs is still lacked until now. This paper is intended to give a brief review of the development of optical-thermal coupled model for PC-LEDs. The review is structured as follows: at first, we discussed the optical model design in PC-LEDs, introduced the influence of the optical parameters in the chips and the phosphor silicone through software simulation in detail. Secondly, we summarized the thermal models to predict the phosphor temperature and the junction temperature. Finally, we summed up optical-thermal coupled model for phosphors and summarized future optical-thermal issues exploring the light quality for LEDs.

## 2 Optical design in PC-LEDs

The radiation of the chips and the emitting light of the phosphor exposed to the ambient after coming through the optical components. Because of the light absorption by the material, it is the key to reduce the optical path of light in the packaging material to improve the LED light efficiency. Therefore, it is necessary to design the structure of each optical element to reduce unnecessary scattering, refraction and total reflection. As for the judgment criteria of the optical element, luminous efficiency, angular color uniformity and color rendering index are crucial to evaluate LED light quality. At present, the influence of the optical components such as the chips and the phosphor silicone matrix was analyzed based on optical ray tracing using the commercial software *ASAP*$^{TM}$ or software *LightTools* and the scattering model. The software support customized device geometries and optical properties such as refractive index, reflectance, transmissivity and scattering properties of each device component. The optical models for LED devices could be divided into two parts: phosphor layer and LED chip, which will be described in details below.

### 2.1 Effect of phosphor parameters on optical properties

Phosphor is a necessary element for LED devices and plays a crucial role in the quality of LED [11]. The phosphor is excited by a high-density photon energy and heat energy from the chips in the circumstance of operating. Due to the heat, the phosphor crystal is in a highly-excited state and results in the LED excitation energy to convert into more thermal radiation via lattice relaxation rather than optical radiation. Such process is known as Stokes shift, thereby further decreasing the luminous efficiency [21,22]. Moreover, the heat energy generated by phosphor is hard to dissipate. Then the phosphor temperature increases greatly and reduces the optical characteristics of phosphor [23]. It has argued that the phosphor temperature is maximum among the temperature distribution [24–26]. Therefore, many researchers made many studies for the phosphor parameters on the optical properties.

#### 2.1.1 Influence of phosphors parameters on angular homogeneity of PC-LED

Angular color uniformity is a key optical property of PC-LEDs. The energy distribution of the blue light emitted by the chip and the yellow light emitted by the phosphor is also different on account of the different luminescent properties of the chip and the phosphor. The different energy distribution eventually leads to a difference in CCT received at different viewing angles. Non-uniformity light color distribution not only reduces the LED quality but also affects the user's feelings. Therefore, the angular color uniformity of the LED must be evaluated.

According to the scattering model of Mie, the scattering process of the model is simulated. Based on the model as illustrated in Fig. 1, the blue LED light is 460 nm and the converted yellow light is 565 nm. Two wavelengths are supposed that only blue light is absorbed and each absorbed blue photon is translated into a yellow photon during the simulation process. To gain the optimized

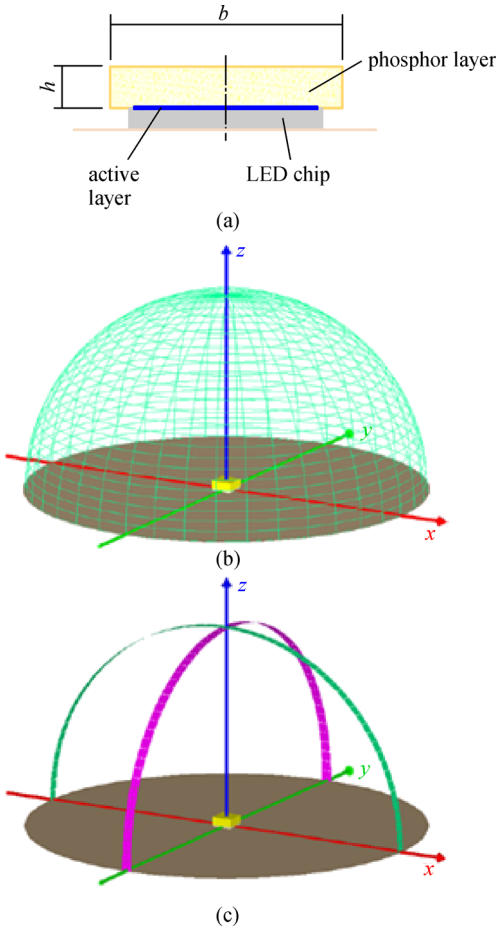


**Fig. 1** Sketch of the simulation model: (a) LED die with a phosphor-layer placed on its top, (b) LED light source with a hemispherical detector, and (c) LED light source with a segmented detector configuration. For the phosphor-layer the height $h$, the width $b$ and the concentration $c$ of the phosphor particles in the silicone matrix are varied throughout the simulations. Both the hemispherical and the segmented detector have a radius of 1 cm. The hemispherical detector is divided into 101 pixels along the principle axes while the segmented detector consists of 61 segments (Adapted from Ref. [27], Copyright 2008, Elsevier)

method of three parameters $h$, $b$, $c$, using control variable method throughout simulation run, namely two of these parameters are kept constant while the third one is varied. The results of ray tracing simulations show that the center of the phosphor layer is more bluish than the border for the lower phosphor-layer heights. With regard to further increased heights, the phenomenon is reversed, namely more yellowish in the center with a bluish fringe at the border. With the phosphor concentration change, the light emission also has a non-homogenous phenomenon which is resemble to the height variation. What is more, the phosphor concentration as an important parameter determines the absorption rate and the scattering rate. It makes the blue LED light initially forward directed radiation properties homogenize [27–30]. Phosphor particles with average diameter of 7.8 μm and a standard deviation of 4.2 μm are regarded as reference particles. A strong deviation from angular homogeneity could be found when particle diameters are varied. Namely, the particle diameter larger than the reference one leads to a yellowish fringe with a bluish center. And the smaller one results in a bluish fringe with a yellowish center. The phenomenon for the larger one could be explained that the blue light is too much forwardly directed and are not in harmony with the converted yellow light. As for the smaller particles, the behavior can be explained that the entire number of phosphor particles per unit volume is comparably larger because phosphor layer having the same phosphor concentration but lower diameters of the phosphor particles. Similarly, the entire number is lower for the larger one. The change in the number of phosphor particles per unit volume is related to the change in the number of scattering events per unit volume. It also denotes that the radiant intensity of both the blue and the converted yellow light is in harmony with the one at different heights of the phosphor layer. Furthermore, it is found that there is a clear correlation giving a straight line between the optimal height and the particle diameter [31–33].

As shown in Fig. 2, three types of surface shapes can be formed by the dispensing process, which is characterized by

$$\text{surface curvature } (\kappa) = \frac{1}{R}\ (\text{cm}^{-1}). \tag{1}$$

$R$ is the radius of the spherical cap. Define $k = 0$, when phosphor layer surface is flat. Meanwhile, $k > 0$ when it is convex and $k < 0$ when it is concave. At the same phosphor concentration, simulation results display that mean CCT reduces with the phosphor surface curvature increases. The amount of phosphor increases with increasing convex surface curvature at the same phosphor density. The increase of phosphor will result in a higher ratio of blue to yellow and a lower mean CCT output. Regarding the situation of the concave phosphor layer surface, the CCT output increases with the total value of the convex surface curvature increase due to the decrease of phosphor amount. The convex phosphor contributes to the light extraction of directional blue light from chips. Compared to the isotropic yellow light of phosphor particles, the convex phosphor comes to higher CCT output and higher ΔCCT. To make the CCT output unchanged, phosphor particle concentration decreases with the surface curvature increases. Yellow and blue light assume angles of 0° and 180° with convex phosphor structures without the typical geometrical boundaries of the reflective cup, resulting in forward light pattern. In addition, the steadiness of the ΔCCT shows that various factors are neutral to each other with the surface curvature increasing. Same ways are used to explain the consequences of concave phosphor structures.

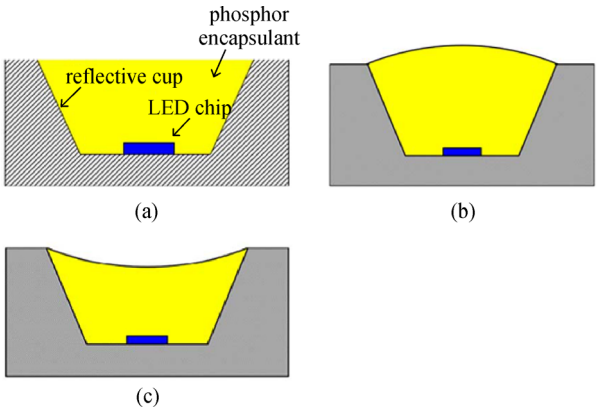


**Fig. 2** Typical structures of in-cup phosphor converted white LEDs (PC-WLEDs) with (a) flat, (b) convex, and (c) concave phosphor layer (Adapted from Ref. [34], Copyright 2011, IEEE)

In contrast to the convex state, the ΔCCT increases as the totally valued of the surface curvature increases because a narrower light escaping cone is formed. The reason for the narrower light escaping cone is the overall internal reflection and the critical angle. As a result, the concave surface curvature prevents light from reaching angles of 0° and 180°. The light extraction is shortened by the surface of the concave phosphor layer. Therefore, for purpose of obtaining superior CCT angular uniformity, the phosphor surface curvature of 3.5 $cm^{-1}$ is chosen as the optimal solution among the LED packages. Liu et al. [80] claimed that the color deviation and YAG:Ce phosphor particle sizes show a linear growth relationship. 2–8 μm particles are more easily to achieve uniform white light than 10–20 μm particles. In other words, 2–8 μm particles is a better choice for high angular color uniformity. If using 10–20 μm particles, it is a good choice to use low phosphor concentration at low color temperature or high phosphor concentration at high color temperature.

To sum up, the manufacture of LED that excel by an optimized angular homogeneity proves to be influenced by lots of factors, including blue LED light source, phosphor concentration, phosphor surface curvature, package types, phosphor-layer thickness and phosphor particle size distribution. All of these factors have to be controlled exactly.

### 2.1.2 Effect of the phosphors parameters on luminous efficacy of PC-LED

As shown in Fig. 3(a), the phosphor layer of in-cup phosphor package is mixed with silicone and phosphor. What is more, the phosphor-silicone mix is dispersed throughout the cup. The remote phosphor package forms a thin phosphor layer which separates from the chip as shown in Fig. 3(b). The outcome shows that the lumen output decreases as the particle size of phosphor increases from nanoparticles to submicron dimensions (between 0.1 and 0.5 μm). Then the luminous flux still increases with the particle size increase to micron size. The cause of this phenomenon is the extent of light scattering. The extent of light scattering is complex in the particle-encapsulant complex material. Moreover, the extent of light scattering is determined by the phase function of particle size, the degree of mismatch in refractive index between particles and encapsulating material, the wavelength and the concentration of particle in suspension. It is common knowledge that nanoparticle composite transmits larger amounts of visible light. It implies that the nanoparticle composite has a low trapping efficiency. Therefore, the luminous flux decreases with the particle size increases from a nano-size to submicron size. In addition, the particle size increase from the submicron size is corresponding to the minimal luminous flux and the complex material produces more transparent to the visible light [34,36,37]. The addition of light transparency diminishes trapping efficiency due to the particles scattering. The luminous flux thus increases with particle size increases from the particle size matching to the minimal luminous flux.

The remote phosphor package (shown in Fig. 3(b)) reduces the amounts of yellow and backscattered light emitted backward into the LED chip. What is more, the luminous flux increases and then decreases with the CCT increases for the two types of packages with the micron

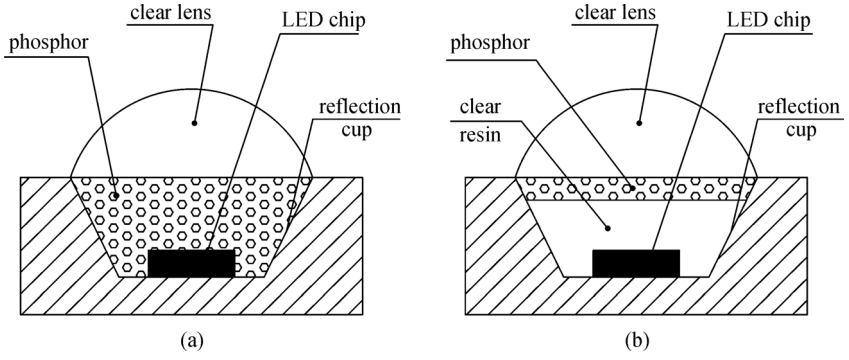


**Fig. 3** Schematic cross-sectional view of PC-WLEDs with (a) in-cup phosphor, (b) top remote phosphor (Adapted from Ref. [35], Copyright 2009, IEEE)

particle size. The reason for the phenomenon is that the luminous flux is a function of the full power and the power distribution of the light spectrum. In the light spectrum with a lower CCT, the power ratio of yellow to blue light is higher. Because yellow light has a higher luminous efficacy than blue one and the luminous efficacy increases as the CCT decreases. To increase luminous efficacy, it is necessary to enhance the phosphor concentration to improve the absorption of blue light and the emission of yellow light by phosphorus particles. The increasing of phosphor concentration results in a raising of trapping efficiency and thus increases the light absorption by packaging materials [38]. When the concentration reaches to a certain value, the light absorption is higher than the positive effect of yellow light on the luminous efficacy. Thus the luminous flux begins to decrease. Higher phosphor thickness has higher luminous flux. And the luminous flux shifts to lower CCT with the addition of phosphor thickness [33]. Under the same conditions for CCT and phosphor size, the luminous flux of the remote phosphor package compared to the in-cup one, is less sensitive to phosphor size and higher [35]. For particle size as a constant, the lumen efficiency increases with the reduction of phosphor concentration because of less light trapping [28]. In addition, the lumen efficiency increased with convex surface curvature due to the improvement of light extraction and the decrease of the phosphor density.

In conclusion, three factors affect lumen output: the relationship between luminous efficiency and wavelength, the phosphor concentration, and the trapping efficiency of phosphor particles. Furthermore, the amount of absorbed blue light increase with phosphor concentration increases, which results in high luminous efficacy. The process of blue light converts to the yellow light makes the luminous efficacy increase because the luminous efficacy of yellow light is higher than the blue one. However, with phosphor concentration increases, the trapping efficiency also increases and becomes a dominant factor at high phosphor concentration [38]. Lower phosphor concentration and higher thickness have lower trapping efficiency and less backscattering of light which lead to the higher luminous efficacy. The luminous efficacy and CCT are strongly influenced by the combination of phosphor concentration, thickness, particles, packages, and so on.

### 2.2 Effect of blue chip

The larger width is compensated by higher phosphor layer due to the blue and yellow light are conducive to white light generation. The blue LED chip has a Lambertian radiation pattern.

$$\theta = \arcsin\left(\frac{n_1}{n_2}\right), \tag{2}$$

where $n_1$ is the refractive index of the low refractive index material, $n_2$ is the refractive index of the high refractive index material, $\theta$ is the critical angle when total reflection occurs. Usually, the refractive index of the chip is about 2.5, and the refractive index of the phosphor powder is about 1.4 and 1.7. The difference between the refractive indexes of the two materials causes the light propagation and the chip-phosphor interface total reflection. According to Eq. (2), the critical angle of total reflection is $34° - 43°$. Therefore, the large lattice mismatch between sapphire and GaN impacts LEDs internal quantum efficiency. And a serious total reflection between sapphire and GaN reduce the light extraction efficiency [39,40]. There are two main methods to improve internal quantum efficiency. One is making epitaxial wafers have low crystal defect density and adopting advanced epitaxial structures. The other one is increasing the carrier radiant recombination-rate and reducing carrier leakage [40–43]. So it is the key to improve light extraction efficiency in various ways, such as patterned sapphire substrate, surfacing roughing. These proposed methods play a significant role in the enhancement of LED luminous efficiency. To find out the optimal methods, researchers have to routinely perform lots of experiments to evaluate the results of varying parameters. However, the manufacturing process and characteristics of LED devices must be performed completely, which is time-consuming and not profitable. In addition, this long process and many steps largely increase the possibility of mistakes, leading to inaccurate and uncertain results. Based on the above disadvantages, a new methodology by computer simulations is hence used in the study.

#### 2.2.1 Chip surface roughening or patterning

Roughening or patterning the top surface of chip is a way to improve the light extraction. The roughed or patterned surface lessens the internal light reflection and outward light scatters [44]. The way to realize surface roughening and patterning includes chemical etching, deposition, etching or printing. The surface of the chip forms a regular or irregular microstructure [44–46]. As shown in Fig. 4, the light can be randomly refracted and reflected at the chip-phosphor interface. More light escapes from the chip and improves the light extraction efficiency of the chip when the chip surface is roughened or patterned. As shown in Fig. 5, Tsai et al. [47] prepared a hemispherical patterned chip surface structure. According to the experimental results, the structure improves the light extraction efficiency by 65% at a driving current of 350 mA compared to the flat chip surface. Cho et al. [45], according to the 3D finite-difference-time-domain (FDTD) simulation, claimed that the extraction efficiency of the PC-LEDs increases steadily with the etch-depth. However, the increment lessens with the etch-depth becomes larger than $\sim\lambda/n$. So the farther optimization of factors such as the lattice constant and the filling factor could pledge the better LEDs.

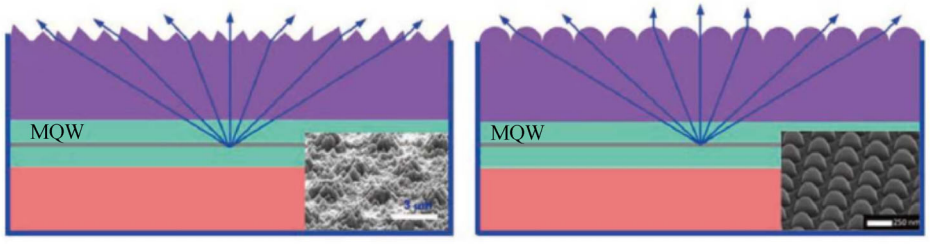


**Fig. 4** Schematic of surface roughening or optical radiation of a patterned chip. (A) Roughening; (b) patterning

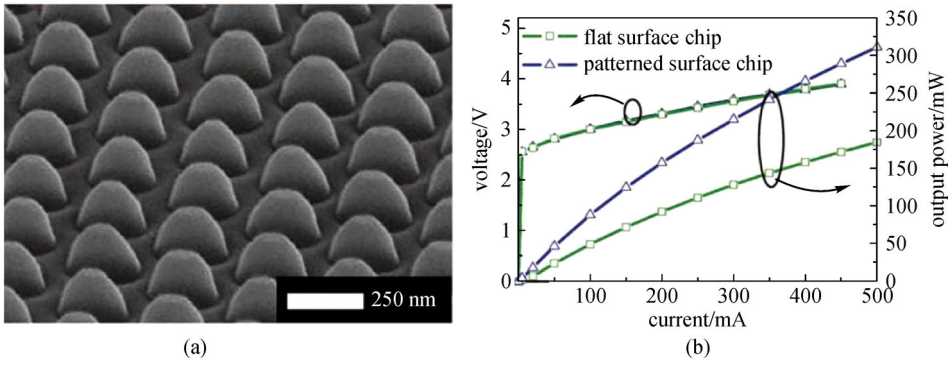


**Fig. 5** Patterned chip surface structure and its light effect to enhance the effect: (a) surface structure; (b) flat surface chip and patterned surface chip luminous efficiency comparison chart

### 2.2.2 Substrate patterning

The basic principle of the substrate patterning is to make a patterned structure on the top surface or the bottom surface of the substrate, for example, a regularly arranged hemispherical array, a columnar array or a conical array [48–50]. As shown in Fig. 6, compared with the flat surface, the patterned substrate can realize the diffuse reflection of the reflected light. Also, the patterned substrate changes the direction and the path of the light propagating so as to improve the light extraction efficiency. *TracePro*, the optical software, is used to run the simulation. The first step of simulation is building the chip model, as shown in Fig. 7. All the parameters are set according to the actual LED devices data to assure the accuracy of the model. The second step is to make the top and bottom surfaces of the "active layer" as Lambertian light sources [40,41]. After setting all the geometry and parameters of the model, *TracePro* will reveal the luminous flux of each surface based on its math function.

Through Wang et al.'s work, various patterned sapphire substrates have been systematically optimized [40]. According to the simulation results, as shown in Fig. 8, the dome-patterned sapphire substrates LED (D-LED) with 10 in the generatrix's central angle exhibits the highest brightness and the lowest luminous intensity. What is more, its total luminous flux is relative high. In addition, as shown in Fig. 9, the EL feature of the chip shows that the luminescence intensity of an optimal dome-patterned sapphire substrates LED is improved 19% compared to the cone-patterned sapphire substrates LED (C-LED) with the same dimensions. These conclusions straightforwardly

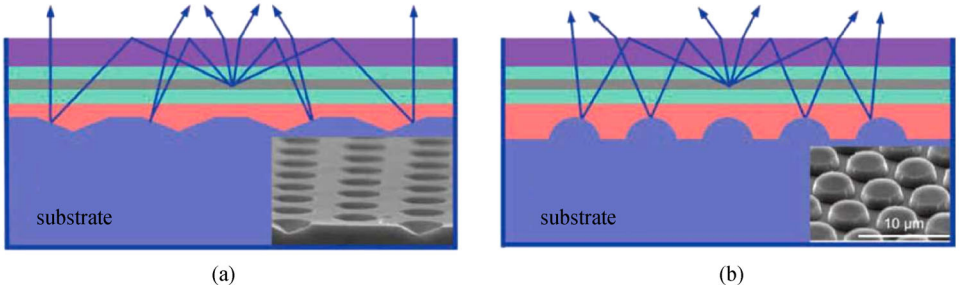


**Fig. 6** Schematic drawing of the substrate. (a) Cone pattern; (b) hemispherical pattern

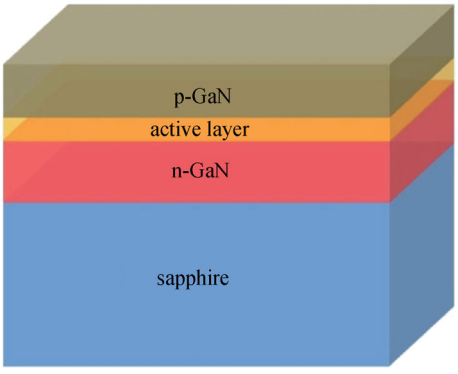


**Fig. 7** Schematic diagram of the LED chip model's structure (Adapted from Ref. [40], Copyright 2015, IOP)

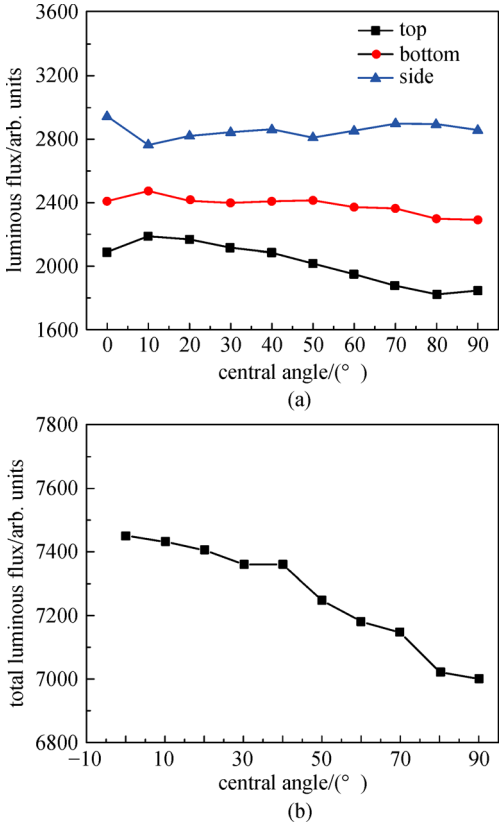


**Fig. 8** (a) Luminous fluxes from each facet and (b) total luminous flux of dome-patterned sapphire substrate (DPSS) LED (Adapted from Ref. [40], Copyright 2015, IOP)

confirm the availability of optimal dome-patterned sapphire substrates for improving LED luminous efficiency [42,43,51–54].

## 3 Thermal design in PC-LEDs

At present, about 65% of the LED input energy is changed into heat. Temperature has a crucial impact on luminous efficacy, lifetime, and color temperature of the LED device and system [55–57]. The heat transfer needs to pass through multiple standards because the LEDs have small size and high power. Thermal design has always been a difficult problem for LED packaging. Besides, the quantum efficiency of LED chips and phosphors are closely related to temperature. So accurately measuring or evaluating LED chip junction temperature and phosphor temperature are the key to thermal design. Heat is generated because of the light absorption and Stokes shift. What is more, the heat increases the chip junction temperature and the phosphor temperature [58–60].

### 3.1 Phosphor temperature

Phosphor temperature will reduce the conversion efficiency, resulting in decrease in the luminous flux, which is called thermal quenching effect [61–63]. The reduction of phosphor emission lows LED lumen efficiency and changes the CCT. In addition, phosphor temperature also causes the peak wavelength shift and the CCT changes [63]. Therefore, it is a challenge to quantify the heat generated in the phosphor layer and analyze how much luminous flux reduces during the LED package. However, the way to measure phosphor temperature is a difficult problem to solve. Thermal model is testified to be an available method to estimate the phosphor temperature. Kang et al. [64] proposed a one-dimensional model for white LED with phosphor layers. The model predicts the blue and yellow light intensities on condition that the phosphor thickness, the boundary's yellow light reflectivity and phosphor particles characteristic parameters are available. But they did not publish details about how to estimate yellow light reflection coefficient for complicated package geometry. Yan et al. [19] found through the simulation that the phosphor temperature is always higher than the chip junction temperature regardless of the position of the phosphor. And the model showed that about 8% of the input energy is changed to heat in phosphor layer. Juntunen et al. [17] proposed a model and considered the heat generated in the phosphor layer. However, this model only laid emphasis on junction temperature estimation and ignored the phosphor temperature calculation.

Three packaging structures are as shown in Fig. 10. The structure for LED chip without any coating has been built unidimensional thermal resistance model, as shown in Fig. 11(I). The model only considers the chip with the die attaches adhesive. The heat transfer path is only from the junction layer to the ambient. As shown in Fig. 11(II), a bidirectional thermal resistance model displays two heat flow branches from the junction to the ambient. The two branches are defined as the upper branch and the lower branch. The lower branch is from junction to the substrate to the ambient. The relevant thermal resistance is $R_{\text{j-s-a}}$. While the upper branch is from the junction pass silicone

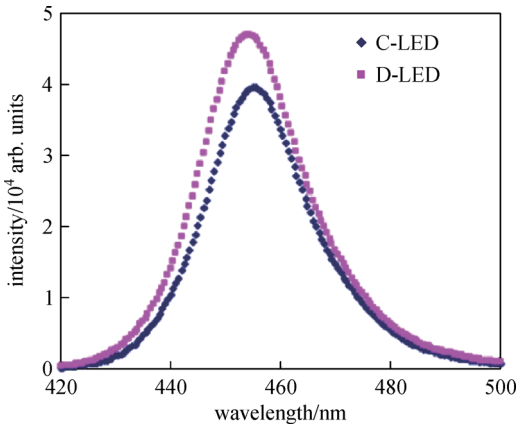


**Fig. 9** EL spectra of LEDs on D-LED and C-LED (Adapted from Ref. [40], Copyright 2015, IOP)

layer to the ambient and the relevant thermal resistance is $R_{sili}$. As for the LED chip with phosphor coating showing in the Fig. 11(III), a modified bidirectional thermal resistance model has two heat source, namely chip heat source $Q_{chip}$ and phosphor heat source $Q_{phos}$. For purpose of evincing the new heat source, the phosphor node $T_{ph}$ is established as the highest temperature in the phosphor layer. Then $Q_{phos}$ is divided into two heat transfer paths. In another word, one is between phosphor node and the ambient $Q_{ph\text{-}a}$ across $R_{ph\text{-}a}$, and the other is between the phosphor node and the junction node $Q_{ph\text{-}j}$ across $R_{ph\text{-}j}$. Therefore, the heat flux part $Q_{ph\text{-}j}$ and $Q_{chip}$ converge into $Q_{j\text{-}a}$, then continues conducting downward to the ambient node [59]. Based on the model, the junction temperature $T_j$ and the phosphor temperature $T_{ph}$ can be acquired as follows:

$$T_j = T_a + R_{1,j\text{-}a} \times Q_{j\text{-}a}, \tag{3}$$

$$T_{ph} = T_a + R_{ph\text{-}a} \times R_{ph\text{-}j}, \tag{4}$$

where $T_a$ is the ambient temperature.

Figure 12 displays the calculated $Q_{phos}$ and $Q_{chip}$ for packaging structure (III) under different driving current. It obviously found that $Q_{chip}$ is always higher than $Q_{phos}$. Namely, most of energy is converted into heat in the chip for PC-LEDs [18]. According to Fig. 13, the $T_{ph}$ is always higher than the $T_j$. Besides, the rising rate of $T_{ph}$ is obviously higher than $T_j$. It means that phosphor temperature is more sensitive compared to the $T_j$. What is more, calculated $T_j$ agrees pretty well with measured $T_j$ by comparing with the simulation and experiment. Figures 12 and 13 verified that a part of energy are converted into heat in the phosphor. As a result, phosphor temperature should be focused on LED package and design process.

An accurate model of PC-LEDs was built in two different ways of package, as shown in Fig. 14. Figure 14(a) revealed phosphor layer is covered on the blue-chip directly; which called direct phosphor coating. Meanwhile, Fig. 14(b) showed the phosphor layer is isolated from chip by silicone encapsulant, which called remote phosphor coating. The phosphor thickness was 80 μm and the ambient temperature was 25°C. In the model, the temperature field was simulated. At the same time, optical simulation was conducted and the light flux absorbed by the phosphor and the chip were calculated.

Figure 15 shows that the heat generation of both the phosphor coating increased significantly with the enhancement of phosphor concentration. The reason for the phenomenon is that more light is absorbed by the phosphor particles with the phosphor concentration increased. The heat generated in chip with direct phosphor coating enhanced. However, the heat generated in the chip with remote phosphor coating hardly changed. Due to the phosphor layer was coated on the chip directly, more blue light emitted from the chip would be back-scattered to the chip, which increased the heat generated by chip. Hence, the heat generated by chip in the direct coating package was higher than the one in remote coating package. Figure 16 demonstrated that as the phosphor concentration increases, the three temperatures in both LED packages increase. The chip temperature is lower than the phosphor temperature and the maximum temperature coincide with the phosphor temperature. It shows that for the direct coating package, the location of hotspot is the phosphor layer, regardless of the phosphor concentration. Since the thermal conductivity of the phosphor is relatively low, the heat in phosphor is hard to be dissipated into the air, so the temperature is slightly higher than that of the chip. For the remote coating package, as shown in Fig. 17, when the phosphor concentration is lower than 0.20 g/cm$^3$, the chip

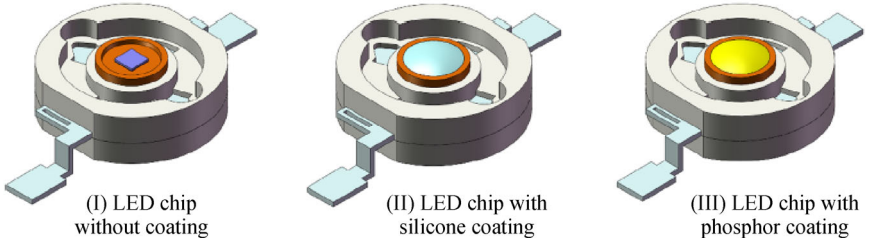


**Fig. 10** Schematic of three LED packaging structures: (I) LED chip without coating, (II) with silicone coating, and (III) with phosphor coating (Adapted from Ref. [18], Copyright 2016, Elsevier)

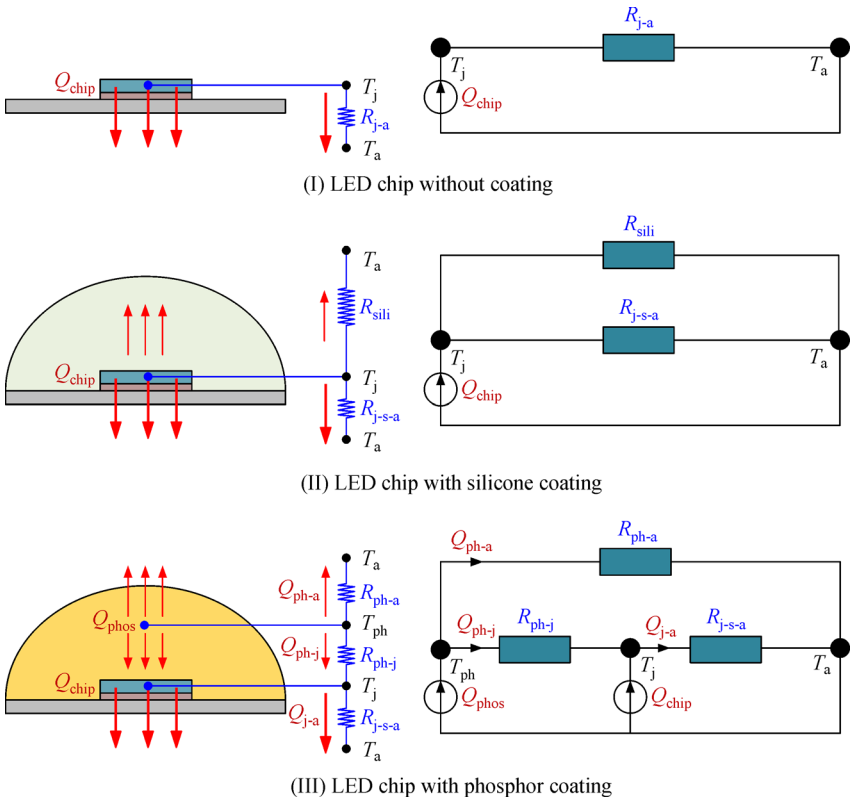


**Fig. 11** Schematic of the heat flow path (left) and the corresponding thermal resistance model (right) for three LED packaging structures (Adapted from Ref. [18], Copyright 2016, Elsevier)

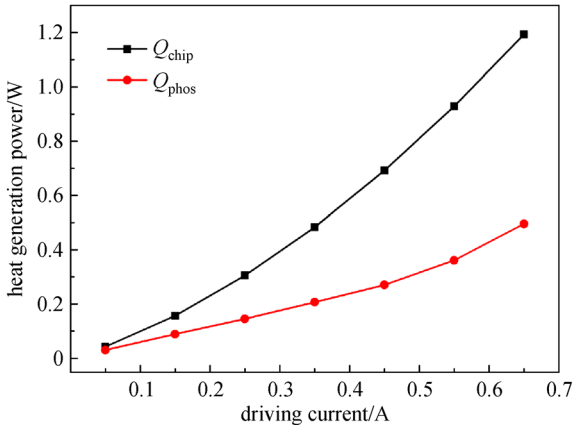


**Fig. 12** Calculated $Q_{chip}$ and $Q_{phos}$ for packaging structure (III) at different driving current (Adapted from Ref. [18], Copyright 2016, Elsevier)

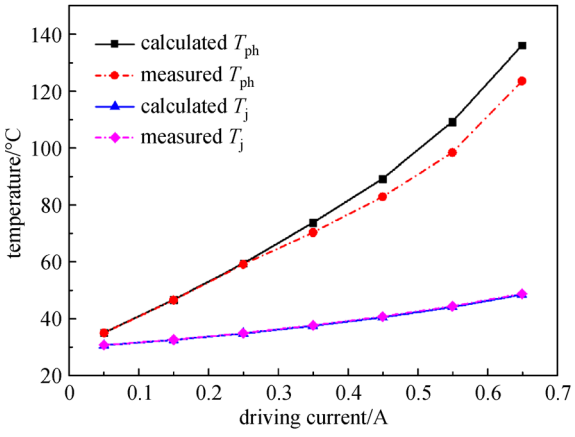


**Fig. 13** Calculated and measured $T_j$ and $T_{ph}$ versus driving current (Adapted from Ref. [18], Copyright 2016, Elsevier)

temperature is higher than the phosphor temperature, the hot spot is on the chip; when the phosphor concentration is over 0.20 g/cm$^3$, the phosphor temperature is higher than the chip temperature, and the hot spot is transferred to the phosphor layer [65].

As shown in the Fig. 18, silicone layer with yellow phosphor coated on blue-chip to produce white light. The phosphor particles have different sizes. In the simulation, the phosphor particles are regarded as two different sizes, 5 and 7 μm, respectively. Based on the above model, the phosphor temperatures of three cases with different phosphor particle configurations were simulated. Figure 19(a) indicated that the larger phosphor particles are in the upper layer of Case 1 and Fig. 19(c) indicated the larger phosphor particles are distributed in the lower layer in Case 3. The larger and smaller phosphor particles are mixed in

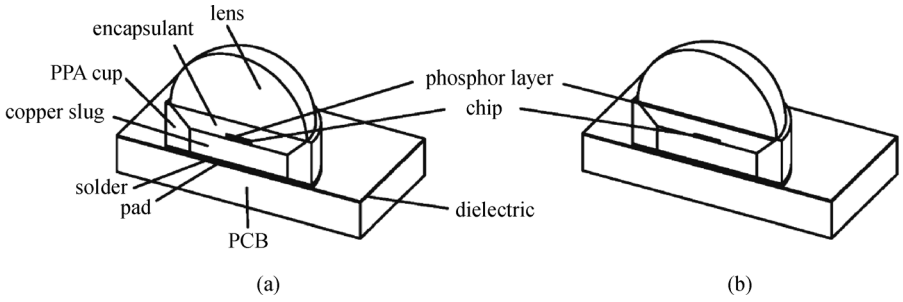


**Fig. 14** Half-3D view of white LED packages with (a) direct phosphor coating and (b) remote phosphor coating (Adapted from Ref. [65], Copyright 2012, The Japan Society of Applied Physics)

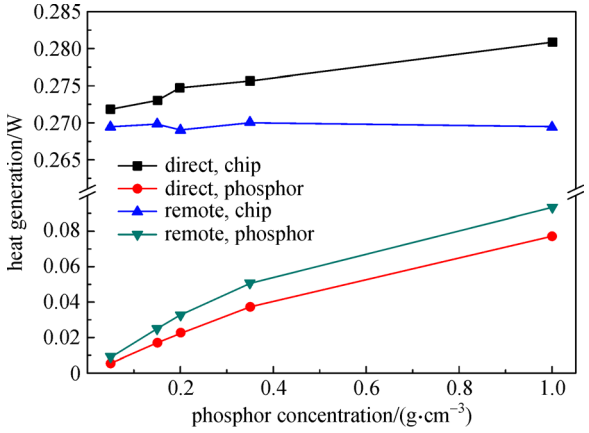


**Fig. 15** Heat generation of the chip and the phosphor layer with different phosphor coatings (Adapted from Ref. [65], Copyright 2012, The Japan Society of Applied Physics)

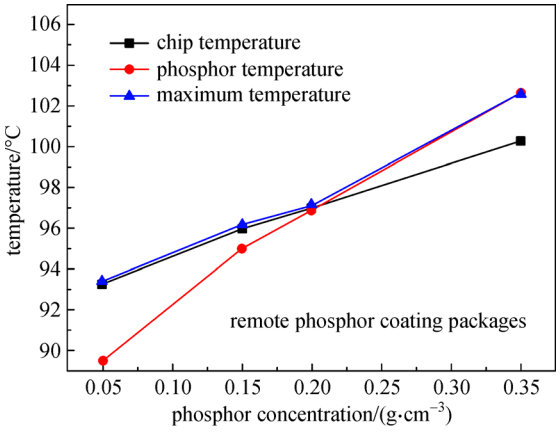


**Fig. 17** Temperature comparisons with the changes in phosphor concentration of LED packages with direct phosphor coating (Adapted from Ref. [65], Copyright 2012, The Japan Society of Applied Physics)

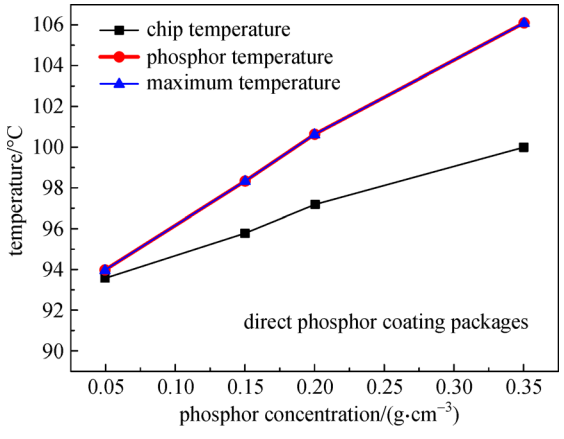


**Fig. 16** Temperature comparisons with the changes in phosphor concentration of LED packages with remote phosphor coating (Adapted from Ref. [65], Copyright 2012, The Japan Society of Applied Physics)

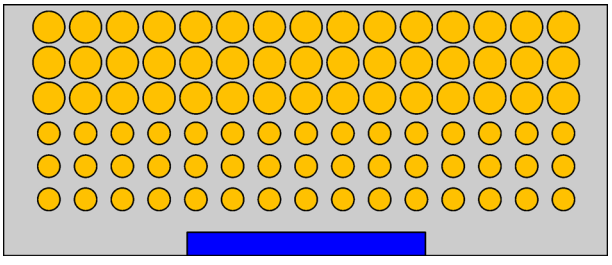

**Fig. 18** Schematic of silicone layer with phosphor particles coated on LED chip. Yellow circles denote the phosphor particles, and blue rectangle denotes the LED chip. The remaining gray part denotes the silicone matrix (Adapted from Ref. [66], Copyright 2014, IEEE)

the Case 2 (see Fig. 19(b)). The simulation result shows that the heat tends to conduct along the phosphor particles due to the phosphors have larger thermal conductivity than the silicone matrix. The phosphor particles which close to the chip have higher temperature and the phosphor particles which is far from the chip have lower temperature. Comparing the phosphor temperatures in the three cases, it is found that the highest temperature in Case 1 is 116.9°C, while he highest temperature in Case 3 is 116.78°C [66]. Case 1 has largest temperature and Case

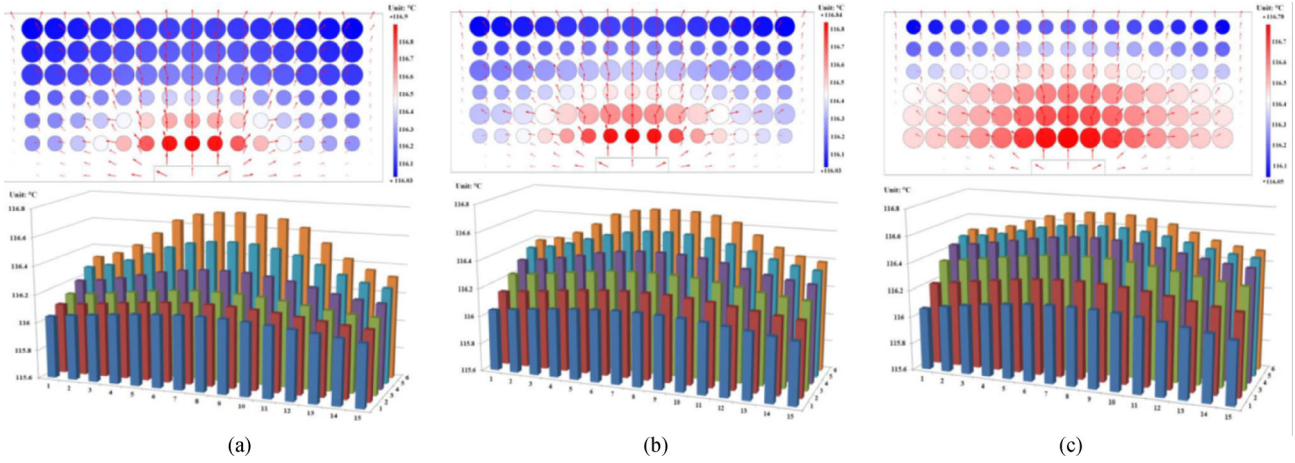


**Fig. 19** Phosphor temperature distribution by FEM simulations and its histogram distribution. (a) Case 1; (b) Case 2; (c) Case 3 (Adapted from Ref. [66], Copyright 2014, IEEE)

3 has lowest temperature. The temperature in Case 2 is the middle one [66]. So the heat is harder to be dissipated into the air for the larger phosphors particles.

### 3.2 Junction temperature

In PC-LEDs, the purpose of continuously reducing the package thermal resistance is to control the temperature of the p-n junction in the LED. As a light emitting device, the junction temperature greatly impacts the performance of the LED. The increase in junction temperature will result in a decrease in the electron-hole recombination probability in the p-n junction. Then the decreasing will affect the chip's internal quantum efficiency and make the brightness of the chip significantly lower after a period of operating [67–69]. As shown in Fig. 20, its optical attenuation speeds up significantly when the junction temperature rises. The higher LED junction temperature will also accelerate the degradation of the packaging material and weak its optical, mechanical, and thermal properties at the package interface, such as yellowing of the silicone, cracks, delamination and so on [70,71]. Further, the degradation of the packaging material makes the LED product reliability decreases and life decreases [72]. Figure 21 shows the relationship between the lifetime of an XLamp XR-E white LED from Cree and the junction temperature. As can be seen from the figure, its service life is significantly reduced when the LED junction temperature rises. In addition, an augment in junction temperature shifts the peaks of LED luminescence and affects the correlated color temperature of the light, resulting in unstable light colors [73].

The model of spiral LED bulb was shown in Fig. 22. Other faces are open boundaries for ambient temperature and environmental pressure. The junction temperature of chips was taken as the monitoring point. Other coefficients

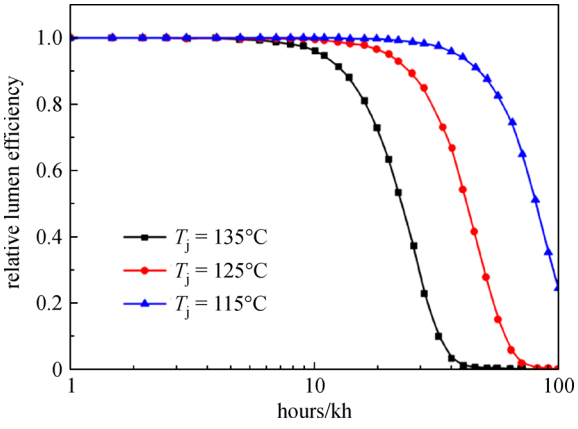


**Fig. 20** Relationship between PC-LED optical attenuation and junction temperature [70]

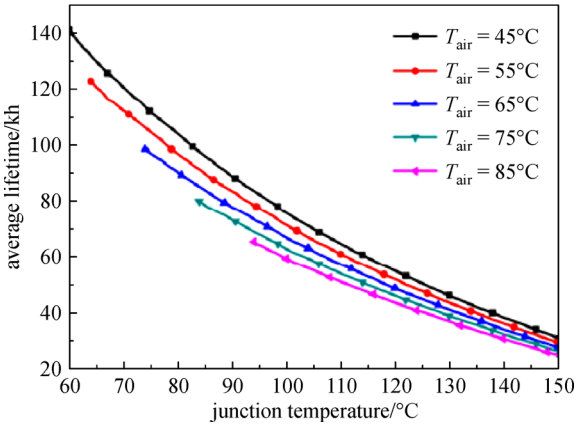


**Fig. 21** Relationship between PC-LED lifetime and junction temperature [70]

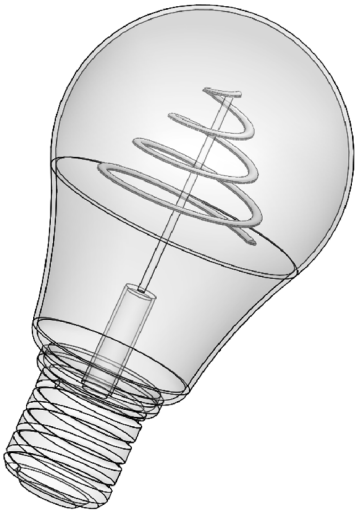

**Fig. 22** Model of spiral LED bulb

of heat transfer could be calculated under the condition of coupling between solid and fluent. The ambient temperature is set as 25°C. According to the color of the filament in Fig. 23(a), the highest temperature was in the center of the spiral PC-LEDs. The temperature gradually decreased with the radius increased. In summary, the shape of flexible LED filament has a great influence on the heat dissipation of flexible LED filament. The chip junction temperature was related to the stretching height closely.

LED junction temperature can be measured in many ways. However, most of them require special instruments or destructive measurement. The measurement process is often complicated and requires a certain amount of time. Therefore, rapid measurement of LED junction temperature by simple measurement is significant. The work in this area has only begun to progress in recent years. Luo et al. [74] proposed a thermal model as shown in Fig. 24, only considering the heat which generated by the chip. Figures 24(b) and 24(c) are the heat flat path and the thermal resistances network, respectively. In this model, $R_{cop}$, $R_{alu,}$ and $R_{TIM}$ respectively represent the thermal resistances of copper heat sink, aluminum stage and TIM layer. $\overline{T}_L$ is the temperature of the bottom surface of the copper heat sink and $h_{equ}$ is the equivalent heat transfer coefficient at the bottom surface of the aluminum stage. The junction temperature is obtained as follows:

$$T_j = h_{equ}A\left(\overline{T}_L - T_a\right)\left(R_{TIM} + R_{alu} + R_{cop}\right) + T_L, \quad (5)$$

where $A$ is the bottom surface of the heat sink. Based on the equitation, it realizes the prediction of the junction temperature of a single LED chip. The copper heat sink in the package bracket was divided into several parts of different diameters for processing. Different parts were connected through the equivalent convection heat transfer coefficient and combined with the measured average temperature of the heat sink fins to realize the prediction of the LED junction temperature. However, in practical applications, there are relatively few products with a single LED as a light source. And it is more common to pack multiple LED chips in an array. The prediction of junction temperature in multi-chip array packages is still in the missing stage.

## 4 Optical-thermal coupled model in PC-LEDs

Heat comes from light and affects light. On the microscopic point of view, luminescence is a radiative transition and heat is a non-radioactive transition. The two factors compete and interact with each other. Actually, the thermal and photometric factors of LED systems are closely linked together. However, most of the existing research studies light and heat alone, ignoring the nature of optical-thermal conversion. Therefore, the optical and thermal aspects of LED devices need to be coupled to study and the light-heat interaction between the photoluminescence was analyzed in depth to improve the light-to-heat conversion efficiency.

Phosphor is a kind of photoluminescence material. The energy conversion process includes radiative transition process and non-radioactive transition process. In the process of radiative transition, phosphor stimulates yellow light while non-radiative transition process generates heat. The energy generated during the non-radiative transition will dissipate in the crystal lattice. The crystal lattice will raise the temperature of the phosphor, resulting in problems such as decreased luminous efficiency and reduced lifetime of the phosphor. Therefore, it is necessary to suppress this non-radiative transition and improve the probability of the occurrence of radiative transitions. The

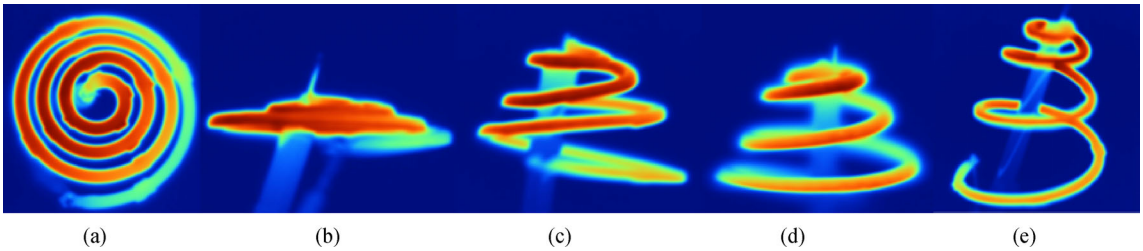

(a) (b) (c) (d) (e)

**Fig. 23** Field distribution at different stretching heights

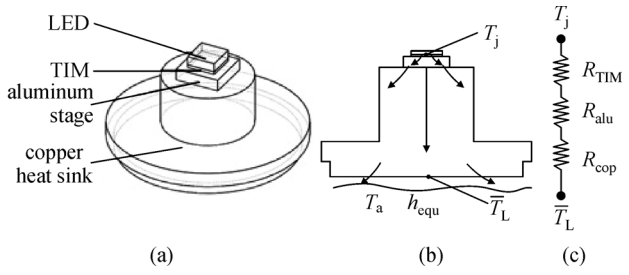


**Fig. 24** Thermal modelling, it is considered that heat generated by the LED chip only conducts through the layers mainly in a direction perpendicular to bottom surface of the copper heat sink. (a) Thermal model; (b) heat flow path; (c) thermal resistances network [74]

radiative transition process and the non-radioactive transition process compete with each other under the premise of energy conservation. And the luminescence and heating processes are coupled with each other. Luo and Hu [75] modified the Kubelka–Munk theory by taking into account the light conversion process during propagation of light in phosphor mixed with silicone. What is more, based on the light scattering model of the phosphor particles, they established a photo-thermal coupling model of phosphor particles and calculated the photo-induced heating of phosphors. They also analyzed the effects of phosphor parameters (thickness, particle size, concentration, conversion efficiency, etc.) on the photo-induced heating of phosphors.

As shown in Fig. 25, the blue and yellow backscattering light energy $F(z)$ can be expressed $F_B(z)$ and $F_Y(z)$. The blue and yellow forward scattering light energy $E(z)$ can be expressed $E_B(z)$ and $E_Y(z)$. $z$ is meant invasion depth and $E_0$ is the input energy. The heat generated by phosphor $Q_{phos}(z)$ could be calculated as follows.

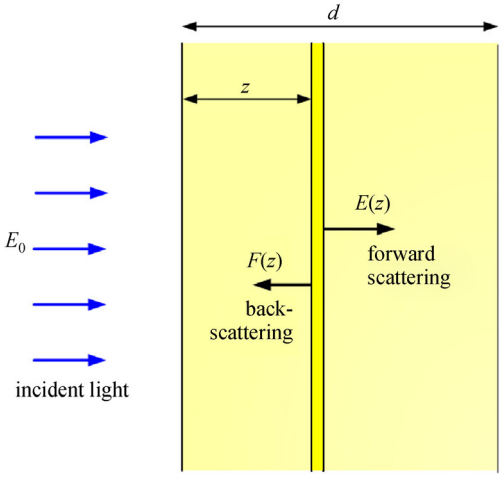


**Fig. 25** Forward scattering and backscattering functions with invasion depth z in a phosphor layer (Adapted from Ref. [75], Copyright 2014, Elsevier)

$$Q_{phos}(z) = (1-\eta_{con})\alpha_B[E_B(z)+F_B(z)] + \alpha_Y[E_Y(z)+F_Y(z)], \quad (6)$$

where $\eta_{con}$ is phosphor particle conversion efficiency, $\alpha_B$ and $\alpha_Y$ are respectively expressed as absorption coefficient of blue and yellow light by phosphor particles. $Q_{phos\_total}$ is defined as the total heat generation, which can be calculated by

$$Q_{phos\_total} = \int_0^d Q_{phos}(z)\mathrm{d}z. \quad (7)$$

It can be seen from Fig. 26 that as the depth of light intrusion increases, the phosphor heat generation is significantly reduced. The phenomenon means that a small invasion depth generates more heat and a large invasion depth generates less heat. The reason for this phenomenon is that the phosphor layer is closer to the chip (a small invasion depth), more light will be scattered, absorbed and converted. Figure 26 can also be found that the phosphor heat generation decreases with the quantum efficiency increases. Namely, more absorbed blue light is changed to yellow light led to less heat. As shown in Fig. 27, the total heat generated in phosphor increase with the addition of phosphor thickness and concentrations. Both two factors have the similar effect on the phosphor heat generation. Above that, phosphor concentration and thickness determine the phosphor amount. In other words, the greater phosphor amount is, more light will scatter, absorb and transform resulting in more heat. As shown in Fig. 28, a peak occurs in the phosphor heat generation and then gradually decreases when the phosphor particles size increases. The peak value corresponds to the critical size of the phosphor. The reason for this critical dimension is that the phosphor scattering coefficient changes with the phosphor particles size [75]. However, by modifying the traditional theory, an optical-thermal coupled model of the phosphor was established to calculate the phosphor heat generation. But their research was limited to the macroscopic level and there was no mutual penetration of optics and thermology into the phosphor photoluminescence and heat generation. Besides, it also lacks research on microscopic energy conversion of phosphors. It is crucial to depth to the microscopic level of the phosphor material, which truly improve the phosphor photoluminescence and heat generation through the material modification. Furthermore, Hui and Qin [76] conducted a theory that connects the electrical, photometric and thermal behaviors of whole LED system. This theory determines the best operating point for an LED system in order to achieve maximum luminous flux for a given thermal design. What is more, the theory demonstrated that thermal design is an integral part of the electrical circuit design. However, the theoretical model is focused on the electrical circuit design. And the

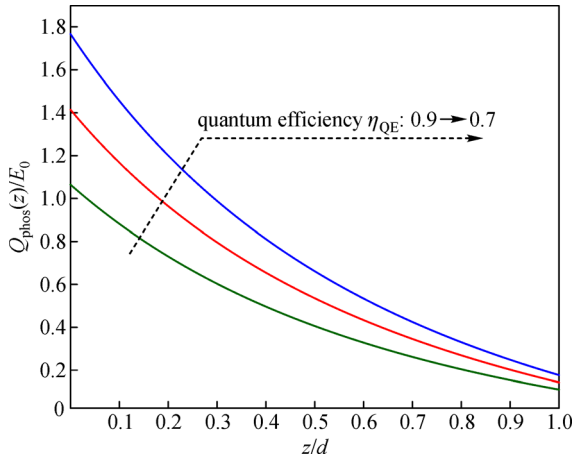


**Fig. 26** Normalized phosphor heat generation function with changing quantum efficiencies

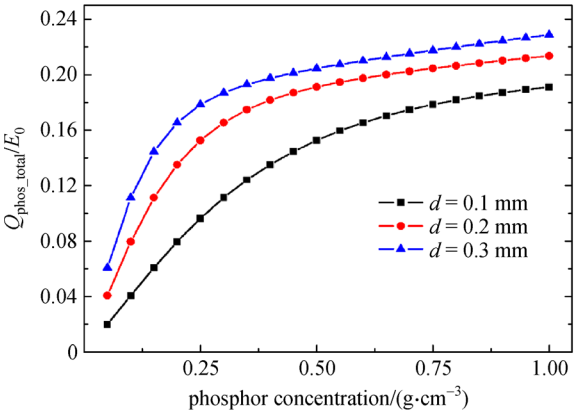


**Fig. 27** Total phosphor heat generation with different concentrations and thicknesses (Adapted from Ref. [75], Copyright 2014, Elsevier)

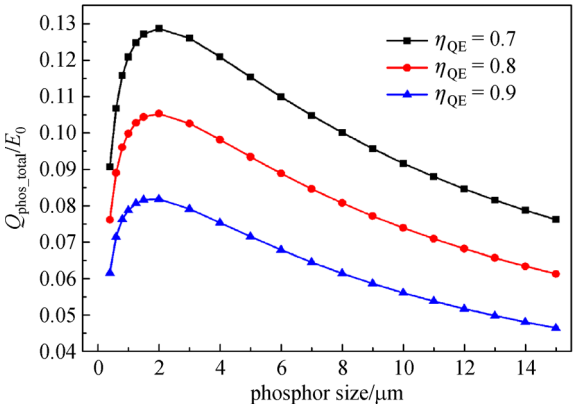


**Fig. 28** Total phosphor heat generation with different phosphor particle sizes and quantum efficiencies (Adapted from Ref. [75], Copyright 2014, Elsevier)

model ignores the phosphor temperature, also not mentioned the relationship between the thermal and optical. Therefore, an LED device model has been established to predict the junction temperature and light output, which ignoring the phosphor temperature [77]. An electrical-thermal-luminous-chromatic model was derived to predict the optical performance with thermal management. It can be used to analyze optical quality and thermal performance due to thickness and particle density variation of phosphors [78].

Ma et al. [79] proposed an optical-thermal coupling model to calculate the phosphor temperature and evaluated the thermal quenching effects of laser-excited remote phosphor by further taking into account the temperature dependence of phosphor quantum efficiency. As shown in Fig. 29, the optical-thermal model consists of phosphor scattering model and settled thermal resistance model. What is more, they are linked through the interaction between phosphor heating power $Q_{ph}$ and phosphor temperature $T_{ph}$. As shown in Fig. 29(a), when the laser beat down on the phosphor layer parallelly, light absorption, conversion and scattering processes happen at the same time. In this situation, four light parts can be derived as forward-scattering and back-scattering energy for yellow and blue light $E_Y(z)$, $E_B(z)$, $F_Y(z)$ and $F_B(z)$, respectively. The overall thermal resistance from the ambient temperature $T_a$ to $T_{ph}$ consist of a series of thermal resistance, as shown in Fig. 29(b), which can be expressed as

$$R_{tot} = R_{ph} + R_{mir} + R_{bond} + R_{hs} + R_{conv}, \tag{8}$$

where $R_{ph}$, $R_{bond}$, $R_{mir}$ and $R_{hs}$ are respectively represented conductive thermal resistance of phosphor layer, bonding layer, mirror layer and heat sink, respectively. $R_{conv}$ is convective thermal resistance from heat sink to the ambient. All heat generated in phosphor layer $Q_{ph}$ can be calculated by the equation as follows:

$$Q_{ph} = P_{in} - P_{out}, \tag{9}$$

$$P_{out} = F_B(0) + F_Y(0). \tag{10}$$

$T_{ph}$ can be calculated by

$$T_{ph} = T_a + Q_{ph}(R_{s,ph} + R_{ph} + R_{mir} + R_{bond} + R_{s,hs} + R_{hs} + R_{conv}), \tag{11}$$

where $R_{s,ph}$ is the relative thermal resistance between pump spot with the plate, $R_{s,hs}$ is the relative thermal resistance between the bonding layer with the heat sink. The temperature dependence of phosphor quantum efficiency $\eta(T_{ph})$, which can be calculated as

$$\eta(T_{ph}) = \frac{\tau_{nr}(T_{ph})}{\tau_{nr}(T_{ph}) + \tau_r}. \tag{12}$$

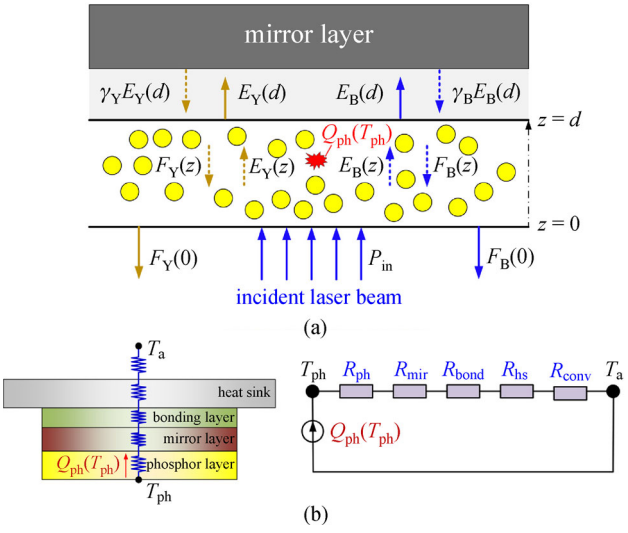


**Fig. 29** Schematic of the optical-thermal model for laser-excited remote phosphor (LERP) comprising (a) phosphor scattering model and (b) thermal resistance model (Adapted from Ref. [79], Copyright 2017, Elsevier)

The temperature dependence of $\tau_{nr}(T_{ph})$ is calculated by

$$\tau_{nr}(T_{ph}) = \frac{1}{W_0}\exp\left(\frac{E_0}{k_B T_{ph}}\right). \quad (13)$$

According to the modified Kubelka–Munk theory and the energy conservation law, the optical-thermal model was calculated step by step as shown in Fig. 30.

The result of simulation shows that coinstantaneous lower phosphor heating and overall thermal resistance are effective to improve Critical incident power $P_{limit}$, and finally enhance the optical-thermal performance of LERPs [79]. However, the optical-thermal coupling model is to study the laser-excited remote phosphor the boundary conditions are not suitable for that of PC-LEDs.

## 5 Conclusion and perspectives

Compared with traditional lamps, white LEDs have the advantages of high luminous efficiency, environmental protection, high reliability and long lifetime which have penetrated into our daily life. LED packages based on blue LED chip and yellow phosphors with silicone are the most widely used scheme to produce white light. In this review, we have discussed the optical model and the thermal model for LED devices. First, we discussed the effect of phosphor parameters on optical properties in details via the software simulation. The final optical performance of the phosphor layer is the result of a combination of these parameters: phosphor material, phosphor particle size and particle distribution, phosphor layer concentration, phosphor layer thickness, geometry and spatial location of the phosphor layer. Predictive model is a crucial way to improve the properties of phosphor. To acquire the optimized balance between high color rendition index and luminous efficacy in LED devices, it is needed to explore the balance between the rational phosphor materials and the anticipated luminescence efficiency. The desired emission position and thermal stability need in accordance with the requirements of phosphor. Secondly, we introduced how to improve light extraction efficiency in various ways, such as patterned sapphire substrate, surfacing roughing. However, the design of chip and improve the light extraction efficiency is still a challenge. Because the effects of complicated geometrical characteristics are hardly possible to methodically analyze by experiments only. Thus, computer simulation is a very effective and reliable way to systematically study. Therefore, varieties of novel geometry chips can be optimized and designed with a rational time span. The field of chip with various ways still needs special attention because innovative chip designed by this computer simulation have potential for further enhancement of the light extraction efficiency of LEDs in the near future. Then, the thermal models are

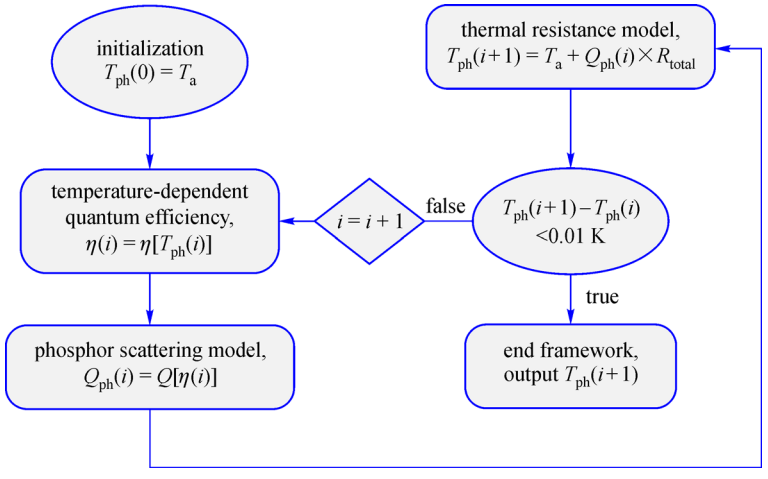


**Fig. 30** Flowchart of the optical-thermal model considering thermal quenching effects (Adapted from Ref. [79], Copyright 2017, Elsevier)

described in details to predict the junction temperature and phosphor temperature. To make the optical performance of PC-LEDs steady, many methods has been made to reduce the junction temperature of the chips. The phosphor temperature as a crucial reliability concern for PC-LEDs should be aroused academic interest. Finally, we summed up optical-thermal coupled model. Looking forward to the future work should pay more attention to the interaction between PC-LED electrons, photons, and phonons to study the transformation between their microscopic energies. Coupling the light and heat of PC-LEDs establish an optical-thermal coupling model and calculate its photo-thermal expression is predictable. There are still many research areas that need further study, including not limited to (1) At present, the packaging technology for single-chip or small-sized LED chip has matured, but the future of LED will inevitably move toward multi-chip high-power integrated development. (2) The new phosphor materials are crucial to the improvement of LED luminous efficiency. The new materials provide the possibility of improving the heat dissipation performance of LEDs. (3) The active layer of the LED chip converts electrical energy into light energy, but a large part of the light energy is absorbed by chips, phosphors, encapsulating glue, and lenses during the propagation process. Therefore, increasing the light extraction efficiency is crucial for the improvement of the photothermal performance of the LED. However, to achieve a major breakthrough in any of the above three aspects, the establishment of an optical-thermal coupled model for LED devices is inseparable, and the mechanism of photo-thermal conversion is studied microscopically.

**Acknowledgements** This work was supported by the Science and Technology Planning Project of Zhejiang Province, China (No. 2018C01046), Enterprise-funded Latitudinal Research Projects (Nos. J2016-141, J2017-171, J2017-293 and J2017-243).

## References

1. Craford M G, Dupuis R D, Feng M, Kish F A, Laskar J. 50th anniversary of the light-emitting diode (LED): an ultimate lamp. Proceedings of the IEEE, 2013, 101(10): 2154–2157
2. Nakamura S, Mukai T, Senoh M. Candela-class high-brightness InGaN/AlGaN double-heterostructure blue-light-emitting diodes. Journal of Applied Physics, 1994, 64(13): 1687–1689
3. Hye Oh J, Ji Yang S, Rag Do Y. Healthy, natural, efficient and tunable lighting: four-package white LEDs for optimizing the circadian effect, color quality and vision performance. Light, Science & Applications, 2014, 3(2): e141
4. Pulli T, Dönsberg T, Poikonen T, Manoocheri F, Kärhä P, Ikonen E. Advantages of white LED lamps and new detector technology in photometry. Light, Science & Applications, 2015, 4(9): e332
5. Kim Y H, Viswanath N S M, Unithrattil S, Kim H J, Im W B. Review—phosphor plates for high-power LED applications: challenges and opportunities toward perfect lighting. ECS Journal of Solid State Science and Technology: JSS, 2018, 7(1): R3134–R3147
6. Pimputkar S, Speck J S, Denbaars S P, Nakamura S. Prospects for LED lighting. Nature Photonics, 2009, 3(4): 180–182
7. Luo X, Hu R, Liu S, Wang K. Heat and fluid flow in high-power LED packaging and applications. Progress in Energy and Combustion Science, 2016, 56: 1–32
8. Tonzani S. Time to change the bulb. Nature, 2009, 459(7245): 312–314
9. Liu S, Luo X. LED Packaging for Lighting Applications: Design, Manufacturing and Testing. Beijing: Chemical Industry Press, Wiley, 2011
10. Gibney E. Nobel for blue LED that revolutionized lighting. Nature, 2014, 514(7521): 152–153
11. Xia Z, Liu Q. Progress in discovery and structural design of color conversion phosphors for LEDs. Progress in Materials Science, 2016, 84: 59–117
12. Langer T, Kruse A, Ketzer FA, Schwiegel A, Hoffmann L, Jönen H, Bremers H, Rossow U, Hangleiter A. Origin of the "green gap": increasing nonradiative recombination in indium-rich GaInN/GaN quantum well structures. Physica Status Solidi (C), 2011, 8(7–8): 2170–2172
13. Correia A, Hanselaer P, Meuret Y. An efficient optothermal simulation framework for optimization of high-luminance white light sources. IEEE Photonics Journal, 2016, 8(4): 1–15
14. Parkyn B, Chaves J, Falicoff W. Remote phosphor with recycling blue-pass mirror. In: Proceedings of SPIE 5942, Nonimaging Optics and Efficient Illumination Systems II. 2005, 59420M
15. Xiao H, Lu Y J, Shih T M, Zhu L H, Lin S Q, Pagni P J, Chen Z. Improvements on remote diffuser-phosphor-packaged light-emitting diode systems. IEEE Photonics Journal, 2014, 6(2): 1–8
16. Tian Y. Development of phosphors with high thermal stability and efficiency for phosphor-converted LEDs. Journal of Solid State Lighting., 2014, 1(1): 11–15
17. Juntunen E, Tapaninen O, Sitomaniemi A, Heikkinen V. Effect of phosphor encapsulant on the thermal resistance of a high-power COB LED module. IEEE Transactions on Components, Packaging and Manufacturing Technology, 2013, 3(7): 1148–1154
18. Ma Y, Hu R, Yu X, Shu W, Luo X. A modified bidirectional thermal resistance model for junction and phosphor temperature estimation in phosphor-converted light-emitting diodes. International Journal of Heat and Mass Transfer, 2017, 106: 1–6
19. Yan B, Tran N T, You J P, Shi F G. Can junction temperature alone characterize thermal performance of white led emitters? IEEE Photonics Technology Letters, 2011, 23(9): 555–557
20. Luo X, Fu X, Chen F, Zheng H. Phosphor self-heating in phosphor converted light emitting diode packaging. International Journal of Heat and Mass Transfer, 2013, 58(1–2): 276–281
21. Sommer C, Reil F, Krenn J R, Hartmann P, Pachler P, Hoschopf H, Wenzl F P. The impact of light scattering on the radiant flux of phosphor-converted high power white light-emitting diodes. Journal of Lightwave Technology, 2011, 29(15): 2285–2291
22. Ishida K, Mitsuishi I, Hattori Y, Nunoue S. A revised Kubelka–Munk theory for spectral simulation of phosphor-based white light-emitting diodes. Applied Physics Letters, 2008, 93(24): 241910

23. Yuan C, Luo X. A unit cell approach to compute thermal conductivity of uncured silicone/phosphor composites. International Journal of Heat and Mass Transfer, 2013, 56(1–2): 206–211
24. Arik M, Weaver S, Becker C, Hsing M, Srivastava A. Effects of localized heat generations due to the color conversion in phosphor particles and layers of high brightness light emitting diodes. In: Proceedings of ASME 2003 International Electronic Packaging Technical Conference and Exhibition. 2003, 611–619
25. Fan B, Wu H, Zhao Y, Xian Y, Wang G. Study of phosphor thermal-isolated packaging technologies for high-power white light-emitting diodes. IEEE Photonics Technology Letters, 2007, 19(15): 1121–1123
26. Hwang J H, Kim Y D, Kim J W, Jung S J, Kwon H K, Oh T H. Study on the effect of the relative position of the phosphor layer in the LED package on the high power LED lifetime. Physica Status Solidi (C), 2010, 7(7–8): 2157–2161
27. Sommer C, Hartmann P, Pachler P, Schweighart M, Tasch S, Leising G, Wenzl F P. A detailed study on the requirements for angular homogeneity of phosphor converted high power white LED light sources. Optical Materials, 2009, 31(6): 837–848
28. Dupuis R D, Krames M R. History, development, and applications of high-brightness visible light-emitting diodes. Journal of Lightwave Technology, 2008, 26(9): 1154–1171
29. Narukawa Y, Narita J, Sakamoto T, Yamada T, Narimatsu H, Sano M, Mukai T. Recent progress of high efficiency white LEDs. Physica Status Solidi, 2007, 204(6): 2087–2093
30. Kim J K, Luo H, Schubert E F, Cho J, Sone C, Park Y. Strongly enhanced phosphor efficiency in GaInN white light-emitting diodes using remote phosphor configuration and diffuse reflector cup. Japanese Journal of Applied Physics, 2005, 44(20–23): L649–L651
31. Sommer C, Krenn J R, Hartmann P, Pachler P, Schweighart M, Tasch S, Wenzl F P. The effect of the phosphor particle sizes on the angular homogeneity of phosphor-converted high-power white LED light sources. IEEE Journal of Selected Topics in Quantum Electronics, 2009, 15(4): 1181–1188
32. Sun C C, Chang Y Y, Yang T H, Chung T Y, Chen C C, Lee T X, Li D R, Lu C Y, Ting Z Y, Glorieux B, Chen Y C, Lai K Y, Liu C Y. Packaging efficiency in phosphor-converted white LEDs and its impact to the limit of luminous efficacy. Journal of Solid State Lighting., 2014, 1(1): 19
33. Kimura N, Sakuma K, Hirafune S, Asano K, Hirosaki N, Xie R J. Extrahigh color rendering white light-emitting diode lamps using oxynitride and nitride phosphors excited by blue light-emitting diode. Applied Physics Letters, 2007, 90(5): 051109
34. Shuai Y, He Y, Tran N T, Shi F G. Angular CCT uniformity of phosphor converted white LEDs: effects of phosphor materials and packaging structures. IEEE Photonics Technology Letters, 2011, 23 (3): 137–139
35. Tran N T, You J P, Shi F G. Effect of phosphor particle size on luminous efficacy of phosphor-converted white LED. Journal of Lightwave Technology, 2009, 27(22): 5145–5150
36. Tran N T, Campbell C G, Shi F G. Study of particle size effects on an optical fiber sensor response examined with Monte Carlo simulation. Applied Optics, 2006, 45(29): 7557–7566
37. Liu Z, Liu S, Wang K, Luo X. Optical analysis of color distribution in white LEDs with various packaging methods. IEEE Photonics Technology Letters, 2008, 20(24): 2027–2029
38. Tran N T, Shi F G. Studies of phosphor concentration and thickness for phosphor-based white light-emitting-diodes. Journal of Lightwave Technology, 2008, 26(21): 3556–3559
39. Liu M, Li K, Kong F, Zhao J, Meng H. Enhancement of the light-extraction efficiency of light-emitting diodes with $SiO_2$ photonic crystals. Optik (Stuttgart), 2018, 161: 27–37
40. Wang H Y, Lin Z T, Han J L, Zhong L Y, Li G Q. Design of patterned sapphire substrates for GaN-based light-emitting diodes. Chinese Physics B, 2015, 24(6): 067103
41. Hiramatsu K, Nishiyama K, Onishi M, Mizutani H, Narukawa M, Motogaito A, Miyake H, Iyechika Y, Maeda T. Fabrication and characterization of low defect density GaN using facet-controlled epitaxial lateral overgrowth (FACELO). Journal of Crystal Growth, 2000, 221(1–4): 316–326
42. Le L, Zhao D, Wu L, Deng Y, Jiang D, Zhu J, Liu Z, Wang H, Zhang S, Zhang B, Yang H. The effects of sapphire nitridation on GaN growth by metalorganic chemical vapour deposition. Chinese Physics B, 2011, 20(12): 400–403
43. Wang C H, Chang S P, Ku P H, Li J C, Lan Y P, Lin C C, Yang H C, Kuo H C, Lu T C, Wang S C, Chang C Y. Hole transport improvement in InGaN/GaN light-emitting diodes by graded-composition multiple quantum barriers. Applied Physics Letters, 2011, 99(17): 171106
44. Fujii T, Gao Y, Sharma R, Hu E L, Denbaars S P, Nakamura S. Increase in the extraction efficiency of GaN-based light-emitting diodes via surface roughening. Applied Physics Letters, 2004, 84 (6): 855–857
45. Cho H K, Jang J, Choi J H, Choi J, Kim J, Lee J S, Lee B, Choe Y H, Lee K D, Kim S H, Lee K, Kim S K, Lee Y H. Light extraction enhancement from nano-imprinted photonic crystal GaN-based blue light-emitting diodes. Optics Express, 2006, 14(19): 8654–8660
46. Xie Z, Zhang R, Fu D, Liu B, Xiu X,Hua X , Zhao H, Chen P, Han P, Shi Y, Zheng Y. Growth and properties of wide spectral white light emitting diodes. Chinese Physics B, 2011, 20(11): 414–416
47. Tsai M A, Yu P, Chiu C H, Kuo H C, Lu T C, Lin S H. Self-assembled two-dimensional surface structures for beam shaping of GaN-based vertical-injection light-emitting diodes. IEEE Photonics Technology Letters, 2010, 22(1): 12–14
48. Lee C E, Lee Y C, Kuo H C, Lu T C, Wang S C. High-brightness InGaN–GaN flip-chip light-emitting diodes with triple-light scattering layers. IEEE Photonics Technology Letters, 2008, 20(8): 659–661
49. Lai F I, Yang J F. Enhancement of light output power of GaN-based light-emitting diodes with photonic quasi-crystal patterned on p-GaN surface and n-side sidewall roughing. Nanoscale Research Letters, 2013, 8(1): 244
50. Su Y K, Chen J J, Lin C L, Chen S M, Li W L, Kao C C. GaN-based light-emitting diodes grown on photonic crystal-patterned sapphire substrates by nanosphere lithography. Japanese Journal of Applied Physics, 2008, 47(8): 6706–6708
51. Hanyoul R. Extraction efficiency in GaN nanorod light-emitting diodes investigated by finite-difference time-domain simulation. Journal of the Korean Physical Society, 2011, 58(41): 878–882
52. Wang H, Zhou S, Lin Z, Qiao T, Zhong L, Wang K, Hong X, Li G. Dome-shaped patterned sapphire substrate with optimized curvature

to enhance the efficacy of light emitting diodes. RSC Advances, 2014, 4(79): 41942–41946
53. Xu S R, Li P X, Zhang J C, Jiang T, Ma J J, Lin Z Y, Hao Y. Threading dislocation annihilation in the GaN layer on cone patterned sapphire substrate. Journal of Alloys and Compounds, 2014, 614: 360–363
54. Wang H, Zhou S, Lin Z, Hong X, Li G. Enhance light emitting diode light extraction efficiency by an optimized spherical cap-shaped patterned sapphire substrate. Japanese Journal of Applied Physics, 2013, 52(9R): 092101
55. Tan S C. General *n*-level driving approach for improving electrical-to-optical energy-conversion efficiency of fast-response saturable lighting devices. IEEE Transactions on Industrial Electronics, 2010, 57(4): 1342–1353
56. Loo K H, Lai Y M, Tan S C, Tse C K. Stationary and adaptive color-shift reduction methods based on the bilevel driving technique for phosphor-converted white LEDs. IEEE Transactions on Power Electronics, 2011, 26(7): 1943–1953
57. Loo K H, Lai Y M, Tan S C, Tse C K. On the color stability of phosphor-converted white LEDs under DC, PWM, and bilevel drive. IEEE Transactions on Power Electronics, 2012, 27(2): 974–984
58. Huang M, Yang L. Heat generation by the phosphor layer of high-power white LED emitters. IEEE Photonics Technology Letters, 2013, 25(14): 1317–1320
59. Hwang J H, Kim Y D, Kim J W, Jung S J, Kwon H K, Oh T H. Study on the effect of the relative position of the phosphor layer in the LED package on the high power LED lifetime. Physica Status Solidi, 2010, 7(7–8): 2157–2161
60. Chen Q, Chen Q, Luo X B. Effect of phosphor layer's location on LED's luminous depreciation under elevated temperature. Chinese Science Bulletin, 2017, 62(12): 1302–1306
61. Bachmann V, Ronda C, Meijerink A. Temperature quenching of yellow $Ce^{3+}$ luminescence in YAG:Ce. Chemistry of Materials, 2009, 21(10): 2077–2084
62. Bachmann V M. Studies on luminescence and quenching mechanisms in phosphors for light emitting diodes. Utrecht University, 2007
63. Tsai C C, Wang J, Chen M H, Hsu Y C, Lin Y J, Lee C W, Huang S B, Hu H L, Cheng W H. Investigation of Ce:YAG doping effect on thermal aging for high-power phosphor-converted white-light-emitting diodes. IEEE Transactions on Device and Materials Reliability, 2009, 9(3): 367–371
64. Kang D Y, Wu E, Wang D M. Modeling white light-emitting diodes with phosphor layers. Applied Physics Letters, 2006, 89(23): 231102
65. Hu R, Luo X, Zheng H. Hotspot location shift in the high-power phosphor-converted white light-emitting diode packages. Japanese Journal of Applied Physics, 2013, 51(9): 994–1000
66. Hu R, Hu J, Luo X. Phosphor temperature reduction by optimizing the phosphor configuration in white light-emitting diode package. In: Proceedings of 14th Intersociety Conference on Thermal and Thermomechanical Phenomena in Electronic Systems (ITherm). 2014
67. Yu T, Shang S, Chen Z, Qin Z, Lin L, Yang Z, Zhang G. Luminescence degradation of InGaN/GaN violet LEDs. Journal of Luminescence, 2007, 122–123: 696–699
68. Arik M, Petroski J, Weaver S. Thermal challenges in the future generation solid state lighting applications: light emitting diodes. In: Proceedings of 8th Intersociety Conference on Thermal and Thermomechanical Phenomena in Electronic Systems (ITherm). 2002
69. Arik M, Becker C A, Weaver S E, Petroski J. Thermal management of LEDs: package to system. In: Proceedings of SPIE 5187, 3rd International Conference on Solid State Lighting. 2004
70. Fu X. Research of junction temperature and phosphor self-heating in LED packaging. Dissertation for the Master Degree. Wuhan: Huazhong University of Science and Technology, 2014
71. Tan L, Li J, Wang K, Liu S. Effects of defects on the thermal and optical performance of high-brightness light-emitting diodes. IEEE Transactions on Electronics Packaging Manufacturing, 2009, 32(4): 233–240
72. Hong E, Narendran N. A method for projecting useful life of LED lighting systems. In: Proceedings of SPIE 5187, 3rd International Conference on Solid State Lighting. 2004
73. Chhajed S, Xi Y, Li Y L, Gessmann T, Schubert E F. Influence of junction temperature on chromaticity and color-rendering properties of trichromatic white-light sources based on light-emitting diodes. Journal of Applied Physics, 2005, 97(5): 054506
74. Luo X, Liu S, Yang J, Mao Z. Engineering method for predicting junction temperatures of high-power light-emitting diodes. IET Optoelectronics, 2012, 6(5): 230–236
75. Luo X, Hu R. Calculation of the phosphor heat generation in phosphor-converted light-emitting diodes. International Journal of Heat and Mass Transfer, 2014, 75: 213–217
76. Hui S Y, Qin Y X. A general photo-electro-thermal theory for light emitting diode (LED) systems. IEEE Transactions on Power Electronics, 2009, 24(8): 1967–1976
77. Baureis P. Compact modeling of electrical, thermal and optical LED behavior. In: Proceedings of 35th European Solid-State Device Research Conference. 2005
78. Ye H, Koh S W, Yuan C, van Zeijl H, Gielen A W J, Lee S W R, Zhang G. Electrical–thermal–luminous–chromatic model of phosphor-converted white light-emitting diodes. Applied Thermal Engineering, 2014, 63(2): 588–597
79. Ma Y, Lan W, Xie B, Hu R, Luo X. An optical-thermal model for laser-excited remote phosphor with thermal quenching. International Journal of Heat and Mass Transfer, 2018, 116: 694–702
80. Liu Z Y, Li C, Yu B H, Wang Y H, Niu H B. Effects of YAG: Ce phosphor particle size on luminous flux and angular color, uniformity of phosphor-converted white LEDs. Journal of Display Technology, 2012, 8(6): 329–335

**Xinglu Qian** received the Bachelor degree from Shanghai Institute of Technology in 2017. And now she is a postgraduate at the Shanghai Institute of Technology. Her major is material chemical engineering. Her current research interests are reliability of LED packaging, mainly involving the research of flexible phosphor film materials and packaging for white LEDs.

**Jun Zou** is currently a professor at the School of Science, Shanghai Institute of Technology. He received his Bachelor degree in inorganic non-metallic materials from Changchun University of Science and Technology in 2002. He obtained his Ph.D. degree in materials science from Shanghai Institute of Optics and Fine Mechanics, Chinese Academy of Sciences in 2007. His research interests include semiconductor materials and devices.

**Mingming Shi** received his Master's degree in materials chemical engineering from Shanghai Institute of Technology in 2016. Now, he is a research assistant at the School of Science, Shanghai Institute of Technology. His current research interests include LED package and simulation.

**Bobo Yang** received his Master's degree in materials chemical engineering from Shanghai Institute of Technology in 2015. Now, he is a research assistant at the School of Science, Shanghai Institute of Technology. His current research interests include phosphor and the application in light emitting diodes.

**Yang Li** obtained her Ph.D. degree in materials science from Shanghai Institute of Optics and Fine Mechanics, Chinese Academy of Sciences in 2018. Now, she is a research assistant at the School of Material Science and Engineering, Shanghai Institute of Technology. Her current research concerns optical glasses and phosphor materials.

**Ziming Wang** is a postgraduate at the Shanghai Institute of Technology. His major is chemical engineering. His current research interest includes LED packaging.

**Yiming Liu** is a postgraduate at the Shanghai Institute of Technology. Her major is material chemical engineering. Her current research interests are optoelectronic materials and devices, mainly involving the research of flexible phosphor film materials and devices for white LEDs.

**Zizhuan Liu** is a postgraduate at the Shanghai Institute of Technology. Her major is material chemical engineering. Her current research interests include spectral coupling law and chromaticity coordinates drift mechanism of LED devices.

**Fei Zheng** is a postgraduate at the Shanghai Institute of Technology. His major is material chemical engineering. His current research interests include semiconductor materials and devices.